www.editada.org

International Journal of Combinatorial Optimization Problems and Informatics, 16(3), May-Aug 2025, 36-45. ISSN: 2007-1558. https://doi.org/10.61467/2007.1558.2025.v16i3.1129

Comparative Analysis of Nonlinear Control Strategies for a Lower Limb Rehabilitation System

Jesús E. Cervantes-Reyes [1], *Ma. De Los Ángeles Alamilla-Daniel*[1], *Ángel Ricardo Lícona-Rodríguez*[1], *Elihu H. Ramirez-Dominguez*[1]
[1]Universidad Politécnica de Pachuca, México.
E-mails: alamillameca@upp.edu.mx

Abstract. Robot-assisted rehabilitation effectively enhances motor recovery in patients with mobility impairments. This study examines the REHAP system—a two-DOF mechatronic rehabilitation device for passive physiotherapy—focusing on dynamic modelling and energy-efficiency analysis. The Euler–Lagrange method was employed to derive the dynamic model, incorporating actuator parameters obtained through experimental characterisation of DC motors. We assessed energy consumption under various control strategies and mechanical-loading conditions. Results indicate that the choice of control strategy and the tuning of actuator parameters significantly impact system efficiency, highlighting the critical need for accurate model calibration. Integrating dynamic modelling improves both motion precision and energy economy, thereby enabling more sustainable rehabilitation technologies. This research underscores how energy-aware control strategies can enhance both performance and sustainability in robotic physiotherapy systems.
Keywords: State feedback control, Adaptive robust control, Sliding mode control, Backstepping control, Lower limb rehabilitation.

Article Info
Received May 3, 2025
Accepted Jul 1, 2025

1 Introduction

The rise in diseases affecting motor skills at both national and international levels has led to a growing demand for rehabilitation across different body extremities, with the lower extremities being the most significant. According to the World Health Organization (WHO) and other health and rehabilitation organizations, this is considered a key aspect of physical development and autonomy across different stages of life (World Health Organization, 2023).

Robotic rehabilitation has emerged as a key tool in the motor recovery of patients with lower limb disabilities, providing assisted therapies that allow repetitive movements with consistent intensity (Han, Wang, Zhang, & Liu, 2022).

The effectiveness of rehabilitation using automatized rehabilitation systems has not been conclusively proven or widely reported in the literature. Our hypothesis suggests that a well-designed system, combined with an appropriately implemented control strategy, can enhance the rehabilitation process by reducing the time required for patient recovery. This highlights the importance of further studies and experimental validation to establish an optimal strategy for their implementation.
Rehabilitation systems can be classified into passive exercises and active exercises. In passive exercises, the rehabilitation system follows a predefined trajectory without patient interaction.

While, in active exercises, the system adapts its movement based on the force exerted by the patient, promoting active participation in therapy (Eiammanussakul & Sangveraphunsiri, 2018).

Robotic rehabilitation systems have incorporated different control strategies to assist patients with reduced mobility. Some systems focus on specific joints, such as TobiBot (Guzmán-Valdivia, Carrera-Escobedo, Blanco-Ortega, Oliver-Salazar, & Gómez-Becerra, 2014), which is designed for ankle rehabilitation. Autor's employ employs a PID control with encoders to manage dorsiflexion and plantarflexion movements, ensuring precision in therapy.

© Editorial Académica Dragón Azteca S. de R.L. de C.V. (EDITADA.ORG), All rights reserved.

Similarly, the parallel system LegUp (Birlescu et al., 2024), designed for rehabilitation in bedridden patients, uses admittance control to regulate the interaction between the robot and the patient, ensuring smooth and appropriate movements.
These systems represent different approaches to robotic re- habilitation, from advanced technologies that adjust assistance in real-time to more direct methods that guarantee stability and safety in therapeutic movements.

The rehabilitation system analyzed in this study, is a robotic system with two degrees of freedom (2-DOF), allowing flexion-extension (Figure 1).

To evaluate its performance, four nonlinear control strategies were implemented: static state feedback, adaptive robust control, sliding mode control, and backstepping control. These control approaches were tested in a simulation environment using MATLAB® to assess their effectiveness in trajectory tracking, stability, and robustness under different conditions, as described in section 2.

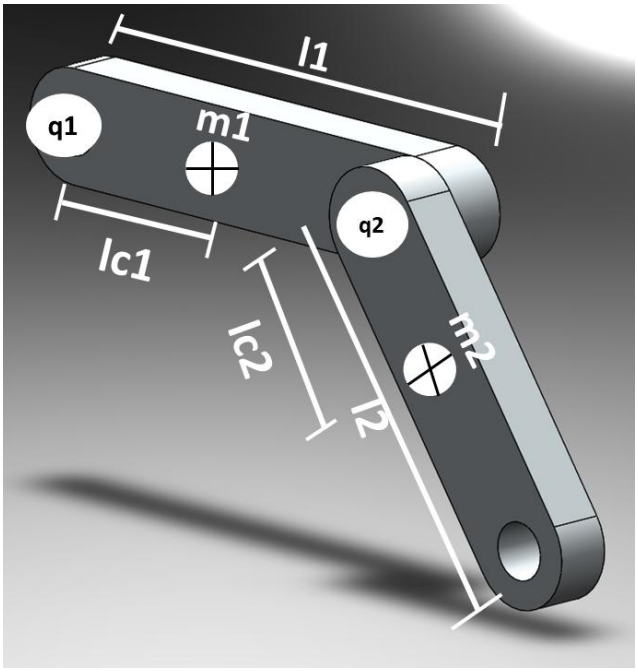

Fig. 1. Two-degree-of-freedom system.

Where:

- q_1 and q_2 are the mechanical system actuators.
- l_1 and l_2 are the links that support the femur and the tibia.
- m_1 and m_2 are the masses of each links.

Its dynamics are modeled using the general equation of robot mechanics:

$$M(q)\ddot{q} + C(q,\dot{q})\dot{q} + G(q) + f(q) = \tau, \quad (1)$$

Source: (Spong, Hutchinson, & Vidyasagar, 2005).

Where:

- q represents the vector of generalized coordinates.
- M (q) is the system's inertia matrix.
- C (q, q̇) is the matrix of centrifugal and Coriolis effects.
- G (q) represents the vector of gravitational forces.
- f (q) represents friction
- τ is the vector of applied torques in the joints.

The inertia matrix M (q) is expressed as:

$$M(q) = \begin{bmatrix} a_{11} & a_{12} \\ a_{21} & a_{22} \end{bmatrix}, \quad (2)$$

Where:

$$a_{11} = m_1 lc_1^2 + m_2(l_1^2 + lc_2^2 + 2l_1 lc_2 \cos(q_2)) + I_1 + I_2$$
$$a_{12} = m_2(lc_2^2 + l_1 lc_2 \cos(q_2)) + I_2$$
$$a_{21} = m_2(lc_2^2 + l_1 lc_2 \cos(q_2)) + I_2$$
$$a_{22} = m_2 lc_2^2 + I_2$$

The Coriolis and centrifugal forces matrix are given by:

$$C(q, \dot{q}) = \begin{bmatrix} -m_2 l_1 lc_2 \sin(q_2)\, \dot{q}_2 & -m_2 l_1 lc_2 \sin(q_2)\,(\dot{q}_1 + \dot{q}_2) \\ m_2 l_1 lc_2 \sin(q_2)\, \dot{q}_1 & 0 \end{bmatrix}, \quad (3)$$

The gravitational force vector is expressed as:

$$G(q) = \begin{bmatrix} (m_1 lc_1 + m_2 l_1) g \cos(q_1) + m_2 g lc_2 \cos(q_1 + q_2) \\ m_2 g lc_2 \cos(q_1 + q_2) \end{bmatrix}, \quad (4)$$

Finally, the friction is expressed as:

$$f\,(q) = \begin{bmatrix} F_{m1} \operatorname{sign}(\dot{q}_1) \\ F_{m2} \operatorname{sign}(\dot{q}_2) \end{bmatrix}, \quad (5)$$

This study presents a comparative analysis of different nonlinear control strategies applied to a 2-DOF rehabilitation system designed for passive kinesitherapy. The four previously mentioned control strategies are implemented and evaluated through simulations and performance index tests, considering key metrics such as accuracy, stability, response time, and robustness against disturbances.

The evaluation will be carried out using performance indices, including the Integral of Squared Error (ISE), Integral of Time-weighted Squared Error (ITSE), Integral of Absolute Error (IAE), and Integral of Time-weighted Absolute Error (ITAE), to quantitatively compare their effectiveness (Dorf & Bishop, 2016).

To evaluate the accuracy and efficiency of the controllers, the following performance index are considered:

- Integral of Squared Error (ISE)

$$ISE = \int_0^T e^2(t)dt \quad (6)$$

  Measures the accumulation of the squared error, prioritizing accuracy by penalizing large deviations.

- Integral of Time-weighted Squared Error (ITSE)

$$ITSE = \int_0^T t\, e^2(t)dt \quad (7)$$

  Similar to ISE, but weights errors over time, favoring fast and stable responses.

- Integral absolute error (IAE)

$$IAE = \int_0^T |e(t)|dt \quad (8)$$

Evaluates the accumulated absolute error without highlighting peaks, making it useful for measuring control effort.

- Integral of Time-weighted Absolute Error (ITAE)

$$ITAE = \int_0^T t\,|e(t)|dt \tag{9}$$

Penalizes prolonged errors over time, reflecting the system's energy efficiency.
ISE and ITSE are key indicators of accuracy, while IAE and ITAE are related to energy consumption and control effort.

The results obtained allow the identification of the advantages and limitations of each method, providing criteria for selecting the most suitable controller based on therapeutic requirements. This study contributes to the development of more efficient, personalized and accessible rehabilitation systems, optimizing therapeutic assistance and improving the interaction between the patient and the robotic system.

2 Nonlinear control laws

The following section focuses on the development of the control laws applied to the system.

2.1 Static state feedback (SSF)

The exact linearization control technique is applied to systems with a completely known dynamic model. This methodology involves defining a system output and successively differentiating it until the input appears explicitly in the resulting expression (Spong, Hutchinson, & Vidyasagar, 2005). If the number of required derivatives matches the system's order, the system is considered fully linearizable.

We define the output as:

$$y = q, \tag{2}$$

The first derivate does not contain the input Taking the second derivative of with respect to time:

$$\ddot{y} = \ddot{q} = M(q)^{-1}\big(\tau - C(q,\dot{q})\dot{q} - G(q)\big), \tag{3}$$

In this second derivative, the input appears explicitly, indicating that the relative degree (Spong, Hutchinson, & Vidyasagar, 2005) of the system is 2. This means that two output derivatives are required for the input to directly influence the system.
With the linearized dynamics, a PD controller can be applied directly to the system's joint positions. We define the position error vector as, where is the desired reference.

The desired control law is:

$$v = \ddot{q_d} + K_p e + K_d \dot{e}, \tag{4}$$

The equation complete is:

$$M(q)\ddot{q} + C(q,\dot{q})\dot{q} + G(q) = M(q)\big(\ddot{q_d} + K_p e + K_d \dot{e}\big) + C(q,\dot{q})\dot{q} + G(q), \tag{5}$$

Simplify:

$$\ddot{q} = \ddot{q_d} + K_p(q_d - q) + K_d(\dot{q_d} - \dot{q}). \tag{6}$$

In Figures (2a) and (2b), the desired vs actual positions are shown for a trajectory following a Bezier curve, as smooth system movements are sought.

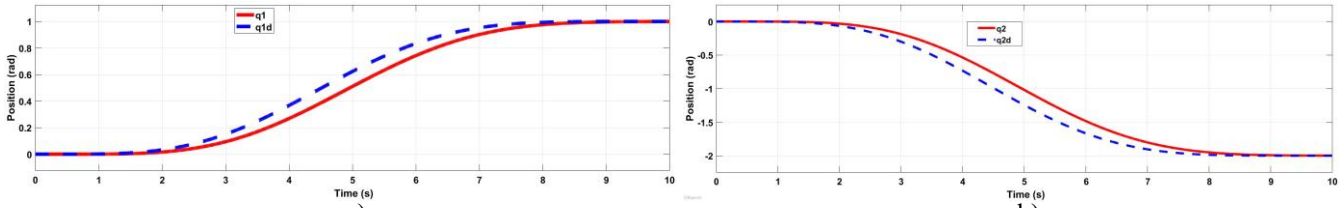

a) b)

Fig. 2. Comparison of the actual vs. desired positions for the two system variables.

Figure 2 shows that the actual trajectory accurately follows the reference trajectory. However, both links exhibit an increase in tracking error as the trajectory curvature increases, which is associated with more abrupt changes in the velocity and acceleration required for accurate tracking.

The following table shows the performance indices for the links.

Table 1. Performance index for the links.

Index	Link 1	Link 2
ITSE	0.001265	0.00008511
ISE	0.0002743	0.00001886
IAE	0.03861	0.009944
ITAE	0.1807	0.04531

This control can only be applied when the exact dynamics of the system to be controlled are known. However, it is not robust to uncertainties or disturbances; therefore, it is not practical for real-world applications.

In the following controllers, an uncertainty will be introduced by increasing the values of masses, lengths, and inertias by 15% to evaluate the robustness of the controller.

2.2 Adaptative robust control (RAC)

The design of RAC ensures stability and desired performance in the presence of disturbances or imprecise modeling (Spong, Hutchinson, & Vidyasagar, 2005). The controller combines a proportional-derivative scheme with an adaptive compensation term to handle uncertainties and nonlinearities (Spong, Hutchinson, & Vidyasagar, 2005).

$$M(q)\ddot{q} + C(q,\dot{q})\dot{q} + g(q) = u, \tag{7}$$

Also, to:

$$u = \widehat{M}(q)a_q + \hat{C}(q,\dot{q})\dot{q} + \hat{g}(q), \tag{8}$$

$$a_q = \ddot{q^d}(t) + K_P(q^d - q) + K_D\left(\dot{q^d} - \dot{q}\right) + \delta a, \tag{9}$$

Defined δ_a as:

$$\delta_a = \begin{cases} -\rho(e,t)\dfrac{B^T Pe}{|B^T Pe|} & \text{si } |B^T Pe| >, \\ -\dfrac{\rho(e,t)}{\epsilon}B^T Pe & \text{si } |B^T Pe| \leq \epsilon \end{cases} \tag{10}$$

In Figures (3a) and (3b), the desired vs. actual positions are shown for a trajectory following a Bezier curve.

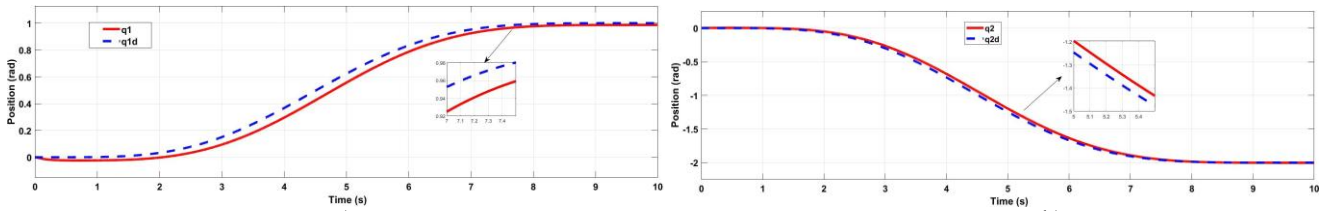

a) b)

Fig. 3. Comparison of the actual vs. desired positions for the two system variables.

Figure 3 shows an improvement in the tracking error, which is more noticeable for link 2, as it demonstrates better performance. According to our hypothesis, this can be attributed to the fact that this link carries a lower load compared to link 1.

The following table shows the performance indices for the links.

Table 2. Performance index for the links.

Index	Link 1	Link 2
ITSE	0.07874	0.03621
ISE	0.01827	0.008142
IAE	0.3739	0.2115
ITAE	1.681	0.9461

2.3 Sliding mode control (SMC)

SMC is a non-linear control technique based on the definition of a surface in the state space, known as the sliding surface, on which the dynamic system is forced to slide (Hernández Zárate, 2015). The objective of SMC is to design u such that the system reaches and remains on a sliding surface σ(x) = 0.

The sliding surface is defined as a scalar function σ(x) that depends on the system states: The sliding surface is generalized as:

$$\sigma\left(x, \dot{x}, \ldots, x^{(n-1)}\right) = \sum_{i=0}^{n-1} \lambda_i \frac{d^i}{dt^i} e \qquad (11)$$

- e = x − xd is the error between the current state x and the desired state xd.
- λ > 0 is a parameter that determines the speed of convergence to the desired state.

The switching functions in SMC are terms in the control law ensure that the system trajectory reaches and remains on the sliding surface. Their main purpose is to enforce the reachability condition, ensuring that the sliding variable σ(x) tends to zero in finite time (Liu, 2017).

The reachability condition in SMC ensures that the system trajectory reaches the sliding surface in finite time (Mantz, 2020).

This is achieved by ensuring that σ'(x) always has a direction opposite to the value of σ(x).

The control law is designed as the sum of two main components:

$$\tau = \tau_{e_q} + \tau_{s_w} \qquad (12)$$

where:

- τ_{e_q} is the equivalent control, which compensates for the system dynamics (direct dynamic model).
- τ_{s_w} is the switching control, which ensures that the system reaches and remains on the sliding surface.

$$\tau_{sw} = -K \tanh\left(\frac{\sigma}{\phi}\right), \quad (13)$$

where K = diag (k1, k2) is a diagonal matrix of switching gains, and ϕ is a parameter that defines the saturation band.

In Figures (4a) and (4b), the desired vs. actual positions are shown for a trajectory following a Bezier curve.

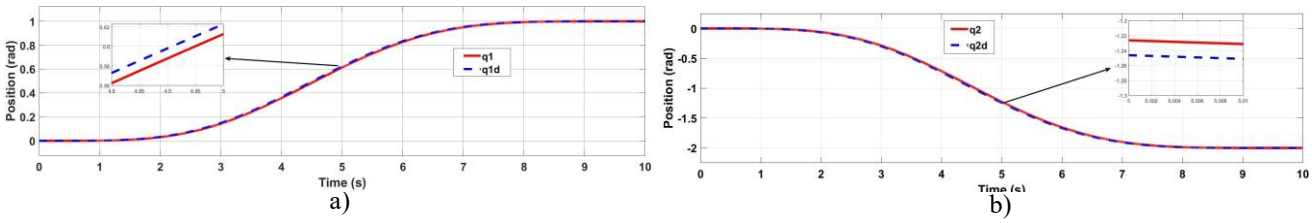

Fig. 4. Comparison of the actual vs. desired positions for the two system variables.

Figure 4 shows a reduction in the tracking error for both links, which is attributed to the controller driving the system states toward asymptotic stability with respect to the reference.

The following table presents the performance indices obtained from the controller.

Table 3. Performance index for the links.

Index	Link 1	Link 2
ITSE	0.001474	0.005546
ISE	0.0003256	0.001222
IAE	0.04227	0.08
ITAE	0.1932	0.3668

2.4 Backstepping control

Backstepping control (BC) is a hierarchical design technique that addresses non- linear systems organized in cascade (Sastry, 1999). By using Lyapunov functions, it aims to stabilize subsystems progressively.

The objective is to design u such that the entire system is asymptotically stable at the origin (Sastry, 1999).
The dynamic error is introduced as:

$$z = \dot{q} - \alpha, \quad (14)$$

$$\dot{z} = \ddot{q_d} - K_1\dot{e} - K_2 z, \quad (15)$$

A virtual control for the joint velocities is proposed as:

$$\alpha = \dot{q_d} - K_1 e, \quad (16)$$

where K1 is a positive diagonal matrix. This control stabilizes the first subsystem:

$$\dot{e} = -K_1 e, \quad (17)$$

Where:

$$\dot{\alpha} = \ddot{q_d} - K_1\dot{e}, \quad (18)$$

We propose the extended Lyapunov function:

$$V_c = \frac{1}{2}e^{\top}K_1 e + \frac{1}{2}z^{\top}M(q)z, \quad (19)$$

Taking the derivative of V_c, we obtain:

$$\dot{V}_c = -e^\top K_1 e - z^\top K_2 z, \tag{20}$$

by selecting the control torque as:

$$M(q)\dot{z} = \tau - C(q,\dot{q})\dot{q} - G(q) - M(q)\dot{\alpha} - f(q), \tag{21}$$

Finally, τ is:

$$\tau = M(q)(\ddot{q_d} - K_1\dot{e} - K_2 z) + C(q,\dot{q})\dot{q} + G(q) + f(q). \tag{22}$$

where K_2 is another positive diagonal matrix.

In Figures (5a) and (5b), the desired vs. actual positions are shown for a trajectory following a Bezier curve.

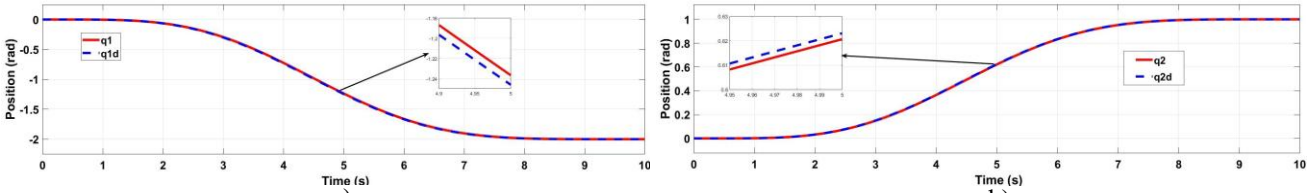

a) b)

Fig. 5. Comparison of the actual vs. desired positions for the two system variables.

Figure 5 shows a slight improvement compared to the SMC controller, as the backstepping controller stabilizes the subsystems sequentially, which contributes to the stabilization of the overall system.

The following table presents the performance index for the links.

Table 4. Performance index for the links.

Index	Link 1	Link 2
ITSE	0.001265	0.00008511
ISE	0.0002743	0.00001886
IAE	0.03861	0.009944
ITAE	0.1807	0.04531

3 Results

To determine the best controller among the four evaluated, the performance indices ITSE, ISE, IAE, and ITAE were compared, as they measure the system's accuracy and efficiency in terms of tracking error. Additionally, the robustness of each controller against uncertainties and disturbances was assessed.

Table 5. Comparison of Performance Indices for Different Controller.

Index	SSF	ARC	SMC	BC
ITSE	0.001265	0.07874	0.001474	0.001265
ISE	0.0002743	0.01827	0.0003256	0.0002743
IAE	0.03861	0.3739	0.04227	0.03861
ITAE	0.1807	1.681	0.1932	0.1807
Robust	✗	✓	✓	✓

These could be presented in tabular or graph form, with appropriate statistical evaluation. Discussion of results. Statement of conclusions drawn from the work.

4 Conclusions

To evaluate the position accuracy of the controllers, the indices ISE (Integral of Squared Error) and ITSE (Integral of Time-weighted Squared Error) were considered. These indices quantify the accumulated trajectory error and penalize prolonged errors, respectively. Lower values in these indices indicate better position accuracy of the system.

The results show that Controllers SSF and BC exhibit the lowest values across all performance indices, indicating that both offer the highest precision in tracking the desired trajectory. However, Controller SSF is not robust, meaning its performance can significantly deteriorate in the presence of disturbances or modeling errors.

In contrast, Controller BC maintains the same level of precision as Controller SSF but is also robust. This implies that it can better adapt to adverse conditions while ensuring stability and good performance, even in situations where the system model is not entirely accurate or when external disturbances are present.
On the other hand, Controllers ARC and SMC exhibit higher performance indices, indicating that they generate greater tracking errors compared to Controllers SSF and BC. Although these controllers are also robust, their lower precision makes them less suitable for the studied application.

Since Controller BC combines the best performance in terms of error with the advantage of robustness, it is concluded to be the best choice for the analyzed system. Its ability to maintain low tracking errors while ensuring stability under uncertainties makes it superior to the other evaluated alternatives.

To evaluate the energy performance of the controllers implemented in the rehabilitation system, various performance indices were analyzed to quantify how efficiently each control strategy minimizes errors and optimizes energy consumption. Among them, the squared error accumulation, the absolute error over time, and indices that weight errors based on time were considered to assess the control effort required at different moments of operation. A lower value in these indices indicates better energy utilization, as it implies that the actuator does not need to exert excessive effort to correct deviations and maintain system stability.

Table 6. Comparison of controllers based on energy efficiency.

Controller	Description
BC	Highest energy efficiency and stability, low control effort.
ARC	Good performance, although with higher consumption than Backstepping.
SMC	Higher control effort, but outstanding robustness.
SSF	Worst energy efficiency, high consumption due to its dependence on the model.

The comparative analysis of nonlinear control strategies applied to a robotic rehabilitation system for lower limbs has identified that BC is the most suitable option to ensure precision, robustness, and energy efficiency in passive rehabilitation therapy. Unlike other evaluated methods, this strategy allows for progressive system stabilization through a hierarchical structure based on Lyapunov functions, ensuring better trajectory tracking with lower sensitivity to disturbances and variations in the system's dynamic model.

For the implementation of the BC in a rehabilitation system, various technical and practical aspects must be considered. Firstly, the dynamic modeling of the system must be well-defined, as this approach requires an accurate mathematical representation of the motion equations to ensure its stability. Additionally, proper tuning of control parameters is necessary, ensuring that gains are optimally selected to balance response speed and error attenuation without compromising system stability. Programming and executing the controller on a robust embedded platform is another key factor, as a processor capable of performing real-time calculations without affecting the mechanical system's performance is required.

From a physiotherapy application perspective, the BC is particularly suitable for assisted passive therapy, in which the patient does not actively intervene in the movement but is instead guided by the system along predefined trajectories with precision. According to our hypothesis, from a physiotherapy application perspective, we consider that the BC is particularly suitable for assisted passive therapy, in which the patient does not actively intervene in the movement but is instead guided by the system along predefined trajectories with precision. This could be particularly useful for the rehabilitation of people with reduced mobility due to neuromuscular disorders, cerebrovascular accidents, or orthopedic injuries.

Furthermore, as a robust and efficient controller, we estimate that it can be applied to systems designed for patients in the early stages of recovery, where ensuring smooth and controlled movements without subjecting the joints to abrupt forces is crucial.

References

World Health Organization. (2023). *Package of rehabilitation interventions*. World Health Organization.

Han, T., Wang, L., Zhang, J., & Liu, X. (2022). Lower limb rehabilitation robots in stroke rehabilitation: An overview of systematic reviews. *Horizons in Rehabilitation, 6*(1), 1–15. https://doi.org/10.31058/j.hr.2021.61001

Eiammanussakul, T., & Sangveraphunsiri, V. (2018). A lower limb rehabilitation robot in sitting position with a review of training activities. *Journal of Healthcare Engineering, 2018*, Article ID 1927807. https://doi.org/10.1155/2018/1927807

Guzmán-Valdivia, C. H., Carrera-Escobedo, J. L., Blanco-Ortega, A., Oliver-Salazar, M. A., & Gómez-Becerra, F. A. (2014). Diseño y control de un sistema interactivo para la rehabilitación de tobillo: TobiBot. *Ingeniería Mecánica, Tecnología y Desarrollo, 5*(1), 255–264. https://www.scielo.org.mx/scielo.php?pid=S1665-73812014000200003&script=sci_arttext

Birlescu, I., Tohanean, N., Vaida, C., Gherman, B., Neguran, D., Horsia, A., Tucan, P., Condurache, D., & Pisla, D. (2024). Modeling and analysis of a parallel robotic system for lower limb rehabilitation with predefined operational workspace. *Mechanism and Machine Theory, 198*, 105674. https://doi.org/10.1016/j.mechmachtheory.2024.105674

Dorf, R. C., & Bishop, R. H. (2016). *Modern control systems* (13th ed.). Pearson.

Spong, M. W., Hutchinson, S., & Vidyasagar, M. (2005). *Robot modeling and control* (1st ed.). John Wiley & Sons.

Liu, J. (2017). *Sliding mode control using MATLAB*. Academic Press.

Hernández Zárate, D. C. (2015). *Sliding mode control for implicit systems* (Doctoral dissertation). Centro de Investigación y de Estudios Avanzados del Instituto Politécnico Nacional.

Mantz, R. J. (2020). *Control por modos deslizantes: Tomo 1. Modos deslizantes de primer orden: Fundamentos y aplicaciones*. Facultad de Ingeniería, Universidad Nacional de La Plata.

Sastry, S. (1999). *Nonlinear systems: Analysis, stability, and control*. Springer.